Structural and Magnetic Properties of Nanocrystalline Copper Ferrites Synthesized by Sol-gel Autocombustion Method

A. S. Padampalle, A. D. Suryawanshi, V. M. Navarkhele, D. S. Birajdar

Abstract— Nanocrystalline copper ferrites are conventionally synthesized by the sol-gel auto combustion method using metal nitrates and citric acid for different temperatures. In this work, X-ray diffractometry (XRD), transmission electron microscopy (TEM), Fourier transform infrared (FT-IR) and vibration sample magnetometry were used to characterize the samples. XRD and selected-area electron diffraction pattern indicates, the synthesized nanocrystalline particles have only the inverse spinel structure without presence of any other phase impurities. Nanocrystalline particles in the range 22-85 nm obtained depending on calcined temperature. FTIR spectra shows, the position of absorption bands are found to be particle size dependent. In magnetic studies, saturation magnetisation increases and coercivity decreases by increasing temperature.

Keywords- Nanocrystalline, $CuFe_2O_4$, X-ray, TEM, FTIR, VSM

I. INTRODUCTION

Nanocrystalline spinel ferrites with general formula MFe_2O_4 (M = Cu, Zn, Mg, Ni, Co etc.) are very important magnetic materials because of their interesting magnetic and electrical properties with chemical and thermal stabilities. These materials have a cubic spinel structure where oxygen forms a face centered cubic close packing and M^{2+} occupy either tetrahedral or octahedral interstitial sites. They provide an opportunity to understand theoretically the interactions at nanoscale. Nanosized ferrites with uniform particle size and narrow size distribution are desirable for variety of applications like targeted drug delivery, ferrofluids, medical imaging and other biomedical applications, medical data storage etc. [1]. Due to their reduced sizes, these nanoparticles may possess novel and improved properties in comparison to bulk materials, which have been extensively used in electronic devices for high frequency telecommunications [2].

The Cu-Fe-O system has been long standing interest in solid-state physics, mineralogy, ceramics and metallurgy. The copper ferrite has two crystallographic spinel structures; the high temperature cubic phase and low temperature tetragonal phase. Since Cu^{2+} is a Jahn-Teller ion, it gives the anomalous favorable properties and also exhibits phase transition from tetragonal to cubic, depending on the temperature. $CuFe_2O_4$ can be described as a cubic close-packed arrangement of oxygen ions, with Cu^{2+} and Fe^{3+} ions at two different crystallographic sites.

Manuscript received on September, 2013.

Dr. A. S. Padampalle, Common Research Facility Center, Shri Chhatrapati Shivaji College Omerga. Dist. Osmanabad, (MS) India.

Dr. A. D. Suryawanshi, Dept. of Physics**,** B.J. College, Ale, Pune (MS) India.

Mr. V. M. Navarkhele, Common Research Facility Center, Shri Chhatrapati Shivaji College Omerga. Dist. Osmanabad (MS), India.

Dr. D. S. Birajdar, Common Research Facility Center, Shri Chhatrapati Shivaji College, Omerga. Dist. Osmanabad, (MS) India.

From a structural standpoint, the formula unit of stoichiometric ferrite can be written as: $(Cu_{\delta}\ Fe_{1-\delta})^{A}\ [Cu_{1-\delta}\ Fe_{1+\delta}]^{B}\ O_4$, where (A) denotes tetrahedral sites, [B] represents octahedral sites [3]. The parameter of inversion, δ is equal to 0 for inverse spinels, and to 1, when the spinel is normal. The temperature of the order-disorder transformation depends on the content of octahedral cupric ions and on the nonstoichiometry [4]. When the spinel is synthesized using ceramic technologies with strict stoichiometry, it has a tetragonal structure of hausmannite type with crystal cell parameters a = 8.20Å and c = 8.60Å; $c/a \sim 1.05$. The c/a ratio can be changed via decreasing the copper concentration, or alternatively by heat treatment temperature and cooling rate [5]. Part of the Cu^{2+} ions can be frozen in tetrahedral sites when the ferrites are quenched in air from above 400°C. The resulting ferrites show a smaller tetragonal distortion since a great proportion of the cupric ions are located on tetrahedral sites.

The nanocrystalline ferrite material is being synthesized by various techniques such as coprecipitation [6], hydrothermal ball milling [7], microemulsion [8], sol-gel method [9] and soon. In the present work, we report the characterization of tetragonal, nanocrystalline copper ferrite using a simple sol-gel autocombustion method which is most suitable for the preparation in good stoichiometric control with narrow particle size distribution in relatively short processing time at lower temperatures.

II. EXPERIMENTAL PROCEDURE

Nanocrystalline copper ferrite was synthesized by a sol-gel auto-combustion method. Copper nitrate ($Cu(NO_3)_2.3H_2O$), ferric nitrate ($Fe(NO_3)_3.9H_2O$ and citric acid ($C_6H_8O_7.H_2O$) were used as starting materials with molar ratio of metal nitrates to citric acid 1:3. All nitrates and citric acid were dissolved in distilled water and stirred continuously. During the constant stirring ammonia solution was added dropwise to adjust PH 7, the solution was heated at 100°C to transform into gel. The gel burnt in a self propagating combustion manner until all gels were completely burnt to form ashes. The as-prepared powder was ground using a mortar and pestle, and then calcined in muffle furnace at 350, 550, 750 950 and 1050°C for 5h and cooled slowly to room temperature.

The calcined samples were characterized for crystal phase identification by powder XRD using Regaku Miniflex II diffractometer with Cu Kα radiation (λ = 1.54056 Å). The particle size and morphology of the calcined powders were characterized by TEM (Philips, CM200).

Published By:
Blue Eyes Intelligence Engineering
& Sciences Publication

Fourier transform infrared (FT-IR) spectra of the powders were recorded using a Fourier transform infrared spectrometer (Bruker) in the range of 4000-200cm^{-1} with resolution of 1cm^{-1}. The magnetic properties of calcined powders were examined using a vibrating sample magnetometer (VSM) at room temperature.

III. RESULTS AND DISCUSSION

XRD patterns of the calcined $CuFe_2O_4$ at five different temperatures between 350 and 1050°C are shown in Fig.1.

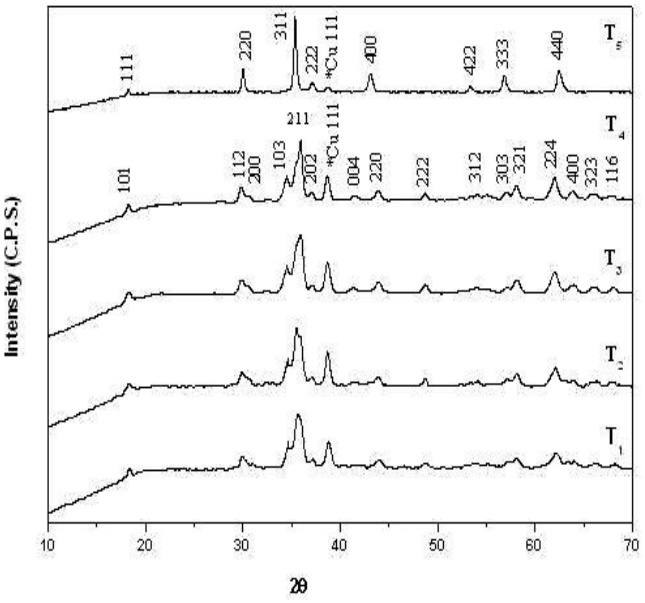

Figure 1X-ray diffraction pattern of $CuFe_2O_4$ sintered at temperature (T_1) 350°C, (T_2) 550°C, (T_3) 750°C, (T_4) 950°C and (T_5)1050°C for 5h.

All the samples calcined up to 950°C exhibit tetragonal symmetry at room temperature. The sample calcined at 1050°C show cubic symmetry at room temperature. It is found that, copper ferrite has tetragonal symmetry up to 950°C and cubic symmetry at and above 1050°C synthesized by autocombustion method. A phase transition from tetragonal to cubic lattice is the result of the disorientation of Jahn-Teller distortions due to a thermal motion of lattice at high temperatures. This transition was found to be influenced by both the distribution of copper ions on the two sublattices and the oxygen non-stoichiometry [10].

All detectable peaks (T_1-T_4) are indexed as $CuFe_2O_4$ with an inverse spinel structure, as shown in the standard data (JCPDS: 340425). The diffraction peak of CuO impurity is observed at diffraction angle 2θ = 38.7°, it is reported by Asbrink and Waskowska et al [11]. In general, the crystal structure of $CuFe_2O_4$ can be either tetragonal or cubic depending on the concentration of Cu ions occupying the octahedral sites. Qi J Q et al [12] reported that, if the system was cooled slowly from high temperature, 88% of Cu^{2+} ions were found to occupy the octahedral site which is a tetragonal distortion of the spinel arrangement. Jiang et al [13] reported that if the Bragg peak at 2θ ≈ 54° appears in all of the XRD patterns, indicating a tetragonal structure in the milled samples. Same symmetry of copper ferrite is reported by D. Thapa et al [14].

The lattice parameters *a* and *c* were calculated from XRD pattern shown in Table I. Both lattice parameters increases with increasing calcined temperature with ratio c/a ≈ 1.47, which represent $CuFe_2O_4$ has tetragonal structure.

Table I
Variation of lattice constant and particle size with temperature for $CuFe_2O_4$ sintered at different temperature.

T °C	Lattice Constant			Particle Size	
	a (A°)	*c* (A°)	*c/a*	t (nm) by XRD	t (nm) by TEM
350	5.8381	8.6283	1.478	22	30
550	5.8616	8.634	1.473	45	60
750	5.8712	8.6419	1.472	66	72
950	5.8722	8.6584	1.474	85	92

The values of lattice parameters *a* and *c* is close (±0.01 Å) to that reported for $CuFe_2O_4$ (*a*= 5.844 and *c*= 8.630 Å) in the standard data (JCPDS: 340425). The linear nature of lattice parameter as a function of temperature can be related to the intrinsic nature of thermal expansion in this alloy as a result of increasing atomic thermal vibrations from their equilibrium positions.

The average particle sizes of $CuFe_2O_4$ samples were calculated from X-ray line broadening the reflections of (220), (222), (321) and (224) using Scherrer's equation ($t = 0.9\lambda / B\cos\theta$), where λ is the wavelength of x-ray radiation, B is full width at half of the intensity maximum of plane in radian and θ is the diffraction angle. The average particle size of the $CuFe_2O_4$ samples were found to be 22, 45, 66 and 85 nm calcined at 350, 550, 750 and 950°C respectively as shown in table I. The size of the particle is observed to be increasing linearly with sintering temperature. While sintering generally lattice defects and strains decreases; it can cause coalescence of the crystallites that result in increasing the average size of particles [15].

The morphology and structure of the powders were investigated by transmission electron microscopy. Fig.2 (a) and (b) shows the TEM image and the corresponding electron diffraction pattern of $CuFe_2O_4$ powder sintered at 350°C and 950°C respectively. It is clearly seen from the TEM bright field images that the morphology and size of the materials were significantly affected by sintered temperature. The $CuFe_2O_4$ sample sintered at 350°C contains well-dispersed nanoparticles with size of <50 nm, where as the $CuFe_2O_4$ sample sintered at 950°C contains of particles of > 100 nm diameter.

Published By:
Blue Eyes Intelligence Engineering
& Sciences Publication

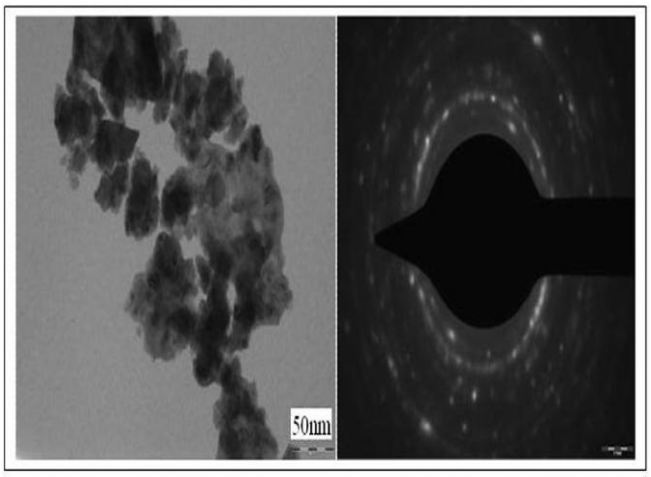

Figure 2 (a) TEM images with corresponding electron diffraction patterns of nanocrystalline $CuFe_2O_4$ samples sintered at temperature 350°C for 5h.

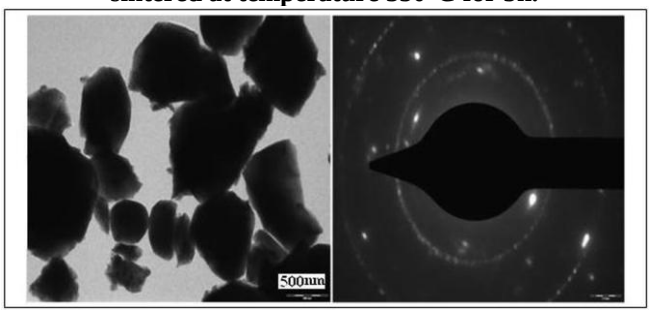

Figure 2 (b) TEM images with corresponding electron diffraction patterns of nanocrystalline CuFe2O4 samples sintered at temperature 950°C for 5h.

The corresponding selected area of electron diffraction patterns of all the $CuFe_2O_4$ shows spotty circular ring patterns without any additional diffraction spots and rings of second phases revealing their crystalline spinel structure. An increase in sintering temperature results in a stronger spotty pattern and the $CuFe_2O_4$ sample shows the strongest spotty patterns, indicating a highly crystalline spinel structure with a large particle size. The particle size distribution is in good agreement with the particle size estimated by Scherrer formula from XRD data.

Fig.3 (a) shows the FTIR absorption spectra of $CuFe_2O_4$ samples calcined from temperature 350 to 950°C. In the range of 200-800 cm^{-1}, two main metal oxygen bands between 600-400 cm^{-1} is obtained which arises due to vibration of ions in the crystal lattices [16]. According to Hafner [17] and Waldron [18], the higher frequency band corresponds to intrinsic stretching vibrations of metal at tetrahedral site (Fe↔O), where as lower frequency band corresponds to octahedral metal stretching (Cu↔O). Fig. 3(b) shows that the sample calcined at 350ºC has been taken FTIR spectra in the range 400-4000cm^{-1}, there is no absorption bands in spectra for all temperature above frequency bands 600cm^{-1}. This is due to complete elimination of water content and amorphous nature above frequency 600cm^{-1}.

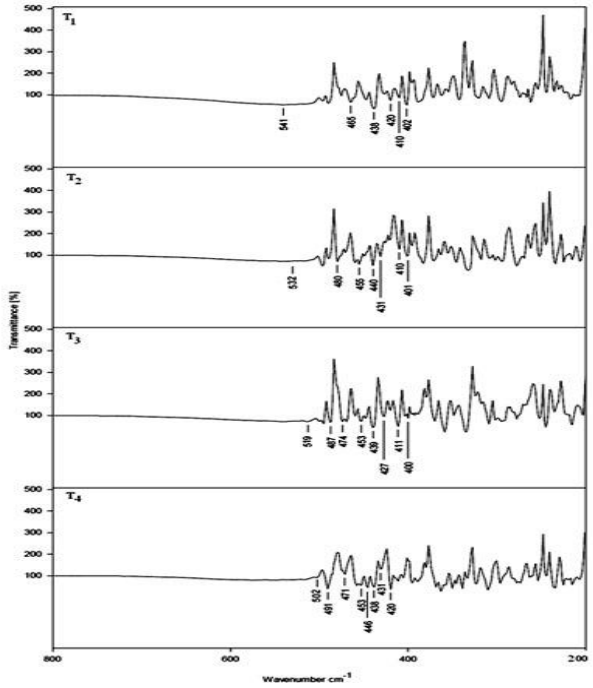

Figure 3(a) FTIR spectra of $CuFe_2O_4$ samples sintered at temperature 350°C to 950°C in the range 200-800 cm^{-1}.

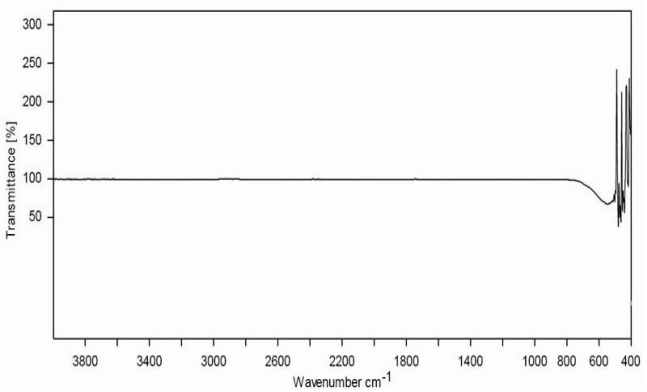

Figure 3(b) FTIR spectra of $CuFe_2O_4$ samples sintered at temperature 350°C in the range 4000-400 cm^{-1}

Table II
Variation of saturation magnetization, coercivity, remnant magnetisation and band position with temperature for $CuFe_2O_4$ sintered at different temperature.

T °C	M_s (emu.g^{-1})	H_c (KOe)	M_r (emu.g^{-1})	Band Position	
				ν_1 cm^{-1}	ν_2 cm^{-1}
350	9.501	1.941	7.439	541	402
550	9.969	1.578	8.263	532	401
750	11.089	2.392	9.541	519	400
950	21.344	0.151	5.694	502	420

The band position of absorption bands are as shown in table II. From table, it is seen that band positions of both bands decreases with increasing calcined temperature. This indicates that band positions are particle size dependent.

Published By:
Blue Eyes Intelligence Engineering
& Sciences Publication

To investigate the influence of the calcined temperature on magnetic properties of $CuFe_2O_4$ samples, hysteresis loops of samples calcined at different temperatures varying from 350 to 950°C were analyzed by VSM, as shown in Figure 4.

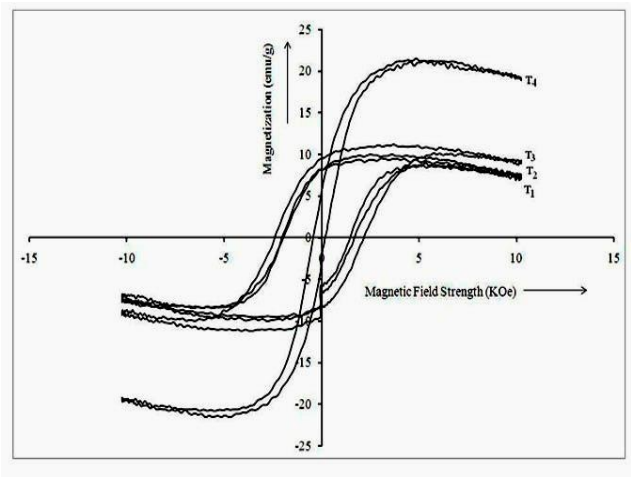

Figure 4 Hysteresis loops of $CuFe_2O_4$ sintered at temperature (T_1) 350°C, (T_2) 550°C, (T_3) 750°C and (T_4) 950°C for 5h.

Also, the corresponding magnetic parameters were listed in Tables II. It can be observed that the values of M_s and M_r were increased by increasing the temperature from 350 to 950°C which arising from spin non-colinearity at the surface of the crystals. The changes in the magnetic properties of the samples can be attributed to the modification of the crystallinity and crystallite sizes dependent on the calcination temperature. The energy of a magnetic particle in the external field is proportional to its particle sizes via the number of molecules in a single magnetic domain. Therefore, the decrease of the M_s values with the decrease of particle sizes can be attributed to surface effects that are the result of finite-size scaling of nanocrystallites [19].

Saturation magnetization increases with increasing temperature which is attributed to the decrease in the inter and intragranular pores resulting from increasing firing temperature. The presence of such pores causes a discontinuity which prevents the movement of domain walls. Remnant magnetic induction shows a very small change with temperature, on the other hand, the coercive force decreases clearly with increasing temperature.

IV. CONCLUSION

In this investigation, it may be concluded that nanocrystalline $CuFe_2O_4$ can be successfully prepared using sol-gel autocombustion method. The samples are calcined by different temperature. Up to temperature 950^0C Cu-ferrite is tetragonal in symmetry and after that it changes to cubic. Particle size increases by increasing calcined temperature. The mean particle diameter between 22 to 85 nm is obtained from XRD and well agreed with TEM data. In FTIR spectra, two main absorption bands are obtained in the frequency range 600-400 cm^{-1} and their positions are particle size dependent. In magnetic studies, by increasing temperature saturation magnetization increases and maximum value is 21.34emu.g^{-1}. The coercivity decreases with increasing temperature.

ACKNOWLEDGMENT

The authors deeply thanks to the head, SAIF, IIT, Bombay for TEM measurement.

REFERENCES

1. S. Deka and P. A. Joy, Mater. Chem. Phys. 100(2006) 98.
2. Z. John Zhang, Z. L. Wang, B. C. Chakoumakos and J. S. Yin, J. Am. Chem. Soc. Vol. 120 No. 8 (1998) 1800.
3. C. Villette, Ph. Tailhades & A. Rousset, *J. Solid State Chem*., 117 (1995) 64.
4. H. Ohnishi & T. Teranishi, J. Phys. Soc. Jpn., 16 (1961), 35.
5. X.X.Tang, A. Manthiram, and J.B. Goodenough, *J. Solid State Chem*., 79 (1989) 250.
6. D. Makovec, A. Kodre, K. Arconjzto ,M. Drofenik, J. Nanopart. Res. 11(2009)1145.
7. A. Ahniyaz, T. Fujiwara, S. W. Song, M. Yoshimura, solid state ionics 151 (2002) 419.
8. A. Kosak, D. Makovec, A. Zindarsic, M. Drofenik, J. Eur. Cream. Soc. 24 (2004)959.
9. P. Kumar, P. Mishar and S. Kumar Sahu, Int. J. Sci. and Eng. Res. Vol. 2 Issue 8 (2011)1.
10. C. Baubet, Ph. Tailhades, C. Bonningue, A. Rousset and Z. Simsa, Journal of Physics and Chemistry of Solids 61 (2000) 863.
11. S. Asbrink and A. Waskowska, J. Phys. Condens. Matter. 3 (1991) 8173.
12. J. Q. Qi, W. P. Chen, M. Lu, Y. Wang, H. Y. Tian, L. T. Li and H. L. W. Chan, nanotechnology 16 (2005) 3098.
13. J. Z. Jiang, G. F. Goya and H. R. Rechenberg, J. Phys. Condens. Matter 11 (1999) 4065.
14. D. Thapa, N. Kulkarni, S. N. Mishra, P. L. Paulose and P. Ayyub, J. Phys. D: Appl. Phys. 43 (2010) 195004.
15. T. P. Raming, A. J. A. Winnubst, C. M. VanKats and P. Philipse, J. Colloid Interface Sci. 249 (2002) 346.
16. V. A. M. Brabers, Phys. Status Solid 33 (1969) 563.
17. S. T. Hafner, Z. Crystallogr. 115 (1961) 331.
18. R. D. Waldron, Phys. Rev. 99 (1955) 1727.
19. Mehrnaz Gharagozlou, chemistry Central Journal (2011) 5.